Preparation of a new chitosan-based material and its application for mercury sorption

Fella-Naouel Allouche, Eric Guibal, Nabil Mameri

Preparation of a new chitosan-based material and its application for mercury sorption

Fella-Naouel Allouche [a,*], Eric Guibal [b], Nabil Mameri [c]

[a] Centre de Développement des Energies Renouvelables, CDER, Laboratoire de Bioénergie et Environnement, BP. 62 Route de l'Observatoire Bouzaréah, 16340-Algiers, Algeria

[b] Ecole des Mines d'Alès, Centre des Matériaux des Mines d'Alès, C2MA/MPA/BCI, 6, Avenue de Clavières, F-30319 Alès Cedex, France

[c] Ecole Nationale Polytechnique, Laboratoire de Biotechnologie Environnementale et Génie des Procédés—BIOGEP, 10, Hacen Badi, El Harrach-Algiers, Algeria

HIGHLIGHTS

- Chitosan sponge-like structure under the form of cylindrical foam has been prepared by freeze-drying technique (holes: Ø: 10 mm; height: 10 mm).
- Preliminary tests, showed that chitosan has relatively a high selectivity to mercury Hg(II).
- pH was the most significant factor that affect the adsorption capacity.
- The application of the cylindrical foam is considered as an encouraging material from laboratory tests to industrial scale.

GRAPHICAL ABSTRACT

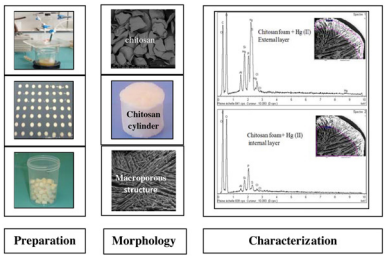

ABSTRACT

A novel chitosan sponge-like structure has been prepared by freeze-drying technique and then tested to remove Hg(II). Chitosan as biosorbent has been used in the form of flakes and cylindrical foams. In this study, column experiment on recirculation mode was conducted in order to determine the sorption properties of the cylindrical foams in various operating conditions (pH, initial metal ion concentration, flow rate, depth of column). The sorption behavior of the materials was examined through equilibrium, kinetic experiments. Hg(II) equilibrium isotherm data is very well fitted by the Langmuir model. Based on the sorption capacity, it was shown that a chitosan flake was more effective than foam. At pH 4, the sorption capacities (qm) were found up to 850 mg of Hg g^{-1} for chitosan flake and only 350 mg of Hg g^{-1} for chitosan foam. Two-region model performed for predicting and determining the sorption capacity of foam were distinguished. The pseudo-second-order chemisorption kinetic has shown success for short sorption times, while the cylindrical diffusion model was able to predict the end of the sorption times. The nature and morphology of the biomaterial before and after mercury sorption was studied by SEM-EDAX analysis.

Keywords:
Chitosan
Foams
Hg(II)
Biosorption
Modeling

1. Introduction

Exposure to heavy metals continues, and is even increasing in the world. Among these heavy metals, mercury Hg(II) is one of the potentially hazardous and toxic element that contaminates our water and air supplies. The World Health Organization con-siders mercury as one of chemical group of great concern to public health, the limit of detection in drinking water is less than 1 μg/L

* Corresponding author. Tel.: +213 663 75 76 03.
E-mail addresses: allouchenaouel2000@yahoo.fr, n.allouche@cder.dz (F.-N. Allouche).

established in 1993 [1]. Considering that poisoning effects arise at the long-term, the perspective on mercury pollution agreed to conduct research effort and developing strategies for reducing the effects of mercury contamination on humans and the environment. The conventional methods for the recovery of heavy metal from industrial effluents have been extensively explored including precipitation, solvent extraction, resins, membrane process and solvent impregnated materials [2]. Based on the ability of various competitive process, many leaders in the industry have become aware of the need for change in industrial process involving classical methods usually carried out on a very large scale. Biosorption process has been proven as good alternative for treatment of various types of effluents containing low metal ion concentration [2,3]. Therefore, the demand for biodegradable materials is ever increasing, which in turn, the application of eco-friendly materials, requires the use of many new kinds of biosorbents such as fungi, [4]; bacteria [5,6]; yeast and algae [7–12]; byproducts [13–15]; . . .etc., for the removal of metals from aqueous solution. In the recent years, special attention has been focused on the use of chitosan as potential biosorbent for removal of heavy metals from wastewater [16–20]. For its natural abundance, more papers have been published since the 1980s in the field of biosorption on chitosan. Most of the applications of chitosan are based on its polycationic nature, acid-base properties, solubility, biocompatibility, biodegradability, non toxicity which allow the use of chitosan for a wide number of applications including food and nutrition, cosmetic, pharmaceutical, biomedical, water treatment and other purposes. However, the presence of amine groups gives to the biopolymer in acidic media a cationic behavior that makes it unique among polysaccharides. These amine groups are responsible for its excellent sorption properties. Nevertheless, chitosan versatility is also the most common property that was used for the preparation of a number of different physical conditioning methods in order to improve the efficiency of the metal sorption capacity. Though, there are many reports on sorption properties of chitosan-based materials in several shapes, in the form of powder, particles and flakes [21,22] and as gels: beads [23,24], films, membranes, [25,26], fibers, hollow fibers [27,28]. In the present work, for comparison, the affinity of the chitosan toward heavy metals including Hg(II), Pb(II), Cd(II), Cu(II), Zn(II), Fe(III) has been studied. Based on the preliminary tests, results showed that chitosan has relatively a high selectivity to mercury Hg(II). Hence, this work aimed to further explore the application of chitosan sponge-like materials as biosorbent for mercury removal from aqueous systems. The main objective of this study includes: (1) first the preparation of chitosan-based materials with porous structure was presented (2) to study the adsorption characteristics of Hg(II) on chitosan-based material; (3) to understand the kinetics (4) and to model the adsorption process.

2. Experiment

2.1. Chemicals

Mercury stock solutions were prepared by dissolving chloride salts of mercury ($HgCl_2$ of Carlo Erba) in demineralized water (Milli-Q). The samples collected during the experiments were filtered through a Millipore membrane (1–2 μm) and then acidified with concentrated nitric acid. Also, all reagents were analytical grade and all solutions were prepared by the dilution of the stock solution in demineralized water (Milli-Q).

2.2. Biosorbents and materials

The chitosan flakes were supplied by ABER Technologies (Plouvien, France). Samples were obtained from the crustacean shells

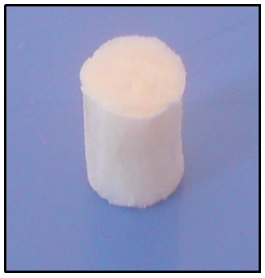

Fig. 1. photograph of chitosan foam.

chitin. The mean particle size range between 1 and 5 mm. The degree of deacetylation was about 87% and an average molecular weight (M_W) was approximately 125,000 g mol^{-1} [29]. Samples used for sorption were ground (JK Crusher, IKA Labortechnik Universal mühle M20) and sieved (sieve Stainless OSI NFX 11504) according to the particle size (PS) distribution, which is prioritized from small to large as: G1 (<125 μm), G2 (125–250 μm), G3 (250–500 μm), G4 (500–710 μm), and G5 (710–1000 μm). In this work, the G2 fraction was used as the reference material.

2.2.1. Chitosan-based material procedure

Granulated chitosan (PS:G2) was initially hydrated before use by stirring in water overnight. The chitosan solution was prepared by adding the polymer in aqueous acetic acid (1%, w/w, 1 g of acetic acid per gram of chitosan G2). The suspension was maintained in agitation for a period of 2 h at ambient temperature for homogeneity and left standing for at least 20 min using a vacuum pump to remove air bubbles. The solution is ready to be used and then poured in lubricated molds (perforated plate formed of cylindrical holes of 10 mm height and 10 mm diameter) that were maintained for 1 h at −80 °C in freezer.

The frozen cylinders formed were rapidly placed overnight in a freeze dried with Alpha 1–4 LD freeze dryer (Christ, Sigma). After 16 h the dried based-material supports were removed from molds and then coagulated overnight at −20 °C into the coagulation bath containing a mixture solution of ethanol/ammonia. Finally, the cylinders supports were rinsed extensively with distilled water and then with ethanol (70% w/w) solution in order to neutralize the excess of ammonia. The cylindrical chitosan foams formed are collected and dried in the open air at ambient temperature (Fig. 1).

2.3. Methods

2.3.1. Batch biosorption studies

2.3.1.1. pH effect. In order to investigate the optimal pH of the metal sorption on chitosan, experiments under controlled pH were carried out by varying initial pH between 2.0 and 7.0. The desired pH was adjusted using a molar solutions of NaOH or H_2SO_4/HCl. The acid was changed to verify if the acid used can impact metal speciation and thus its sorption. Samples containing 0.020 g of chitosan (G2) were added to 100 mL of solution containing aqueous Hg(II) with desired initial concentration and pH value. The flasks were shaken on a reciprocal shaker (150 movements per min) at room temperature for 24 h at 20 °C. The solution was filtrated using a 1–2 μm pore size filtration membrane and the filtrate was analyzed by ICP-AES (Jobin-Yvon Activa-M, Jobin-Yvon, Longjumeau, France) for equilibrium metal concentration (Ceq: mg metal L^{-1}). The amount of Hg(II) uptake by chitosan (q) was determined using the mass balance equation:

$$q = \frac{V(C_0 - C_e)}{m} \quad (1)$$

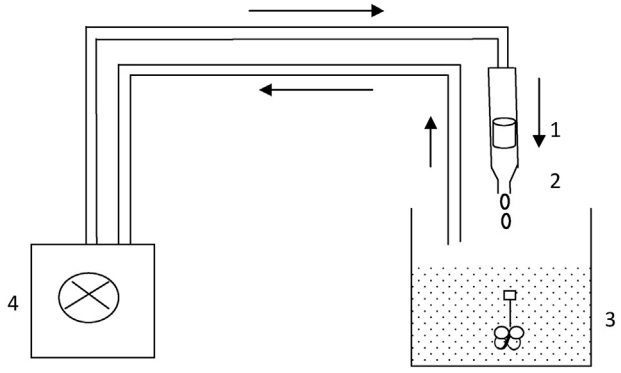

Fig. 2. Schematic representation of laboratory scale batch adsorber vessel. 1 adsorbant (chitosan foam); 2 column; 3 glass tank; 4 peristaltic pump.

where q is the adsorption amount at equilibrium (mg g^{-1}), C_0 and C_e are the initial and the equilibrium concentrations in solution, respectively (mg L^{-1}), while m (g) represents the dry weight of the adsorbent and V (L) is the volume of the solution. The final pH was monitored at equilibrium (WTW pH meter, Model 526 pH, with pH electrode ref. SenTix 41, Germany).

2.3.1.2. Sorption isotherms. The experimental setup for batch system was comparatively performed at pH 4 for both chitosan G2 and chitosan foams under identical operating conditions (approximate mass of 1 foam ≈0.0450 g). The adsorption of Hg(II) was studied by placing a given amount of sorbent into 100 mL of metal solution at the appropriate pH. The initial metal concentration (C_0) was varied between 10 and 200 mg Hg L^{-1}. The samples were kept under stirring at room temperature (20 °C) for 48 h. The solution was filtrated using a 1–2 μm pore size filtration membrane and the filtrate was analyzed by ICP-AES for equilibrium metal concentration (Ceq: mg metal L^{-1}). All experiments were done 3 times and all values of the results were presented as average in this study.

2.3.1.3. Uptake kinetics.

2.3.1.3.1. Batch methods. Kinetic experiments were performed at room temperature (20 °C) by mixing 0.625 g L^{-1} of chitosan G2 at the appropriate pH. The investigation was performed with the initial concentration of Hg(II) range of C_0: 25–50–100 mg Hg L^{-1}. The suspension was maintained under agitation at 200 movements per min. Samples were collected at different contact times, filtrated and analyzed by ICP-AES.

2.3.1.3.2. Column preparation procedure. The experimental setup was carried out, using chitosan foam under the cylindrical form in a fixed bed mini plastic column with an inside diameter of 10 mm. The distilled water was passed through the column to get wet chitosan material. For the determination of optimum conditions, kinetic experiments were performed at a known concentration and flow rate on a recirculation mode. The metal solution was shaken by a magnetic bar and stirrer at the agitation speed of 200 movements per min at a constant temperature (20 °C) and at optimum pH value of 4. The metal solution was re-circulated through the column at constant flow rate using a peristaltic pump. A schematic diagram of the experimental set up was shown in Fig. 2. Samples were collected periodically, and analyzed for mercury concentration by ICP-AES. All experiments were performed according to the general procedure described above.

2.4. Material characterization

Samples of both chitosan (fraction G2) and foams were characterized by Environmental Scanning Electron Microscope (ESEM)

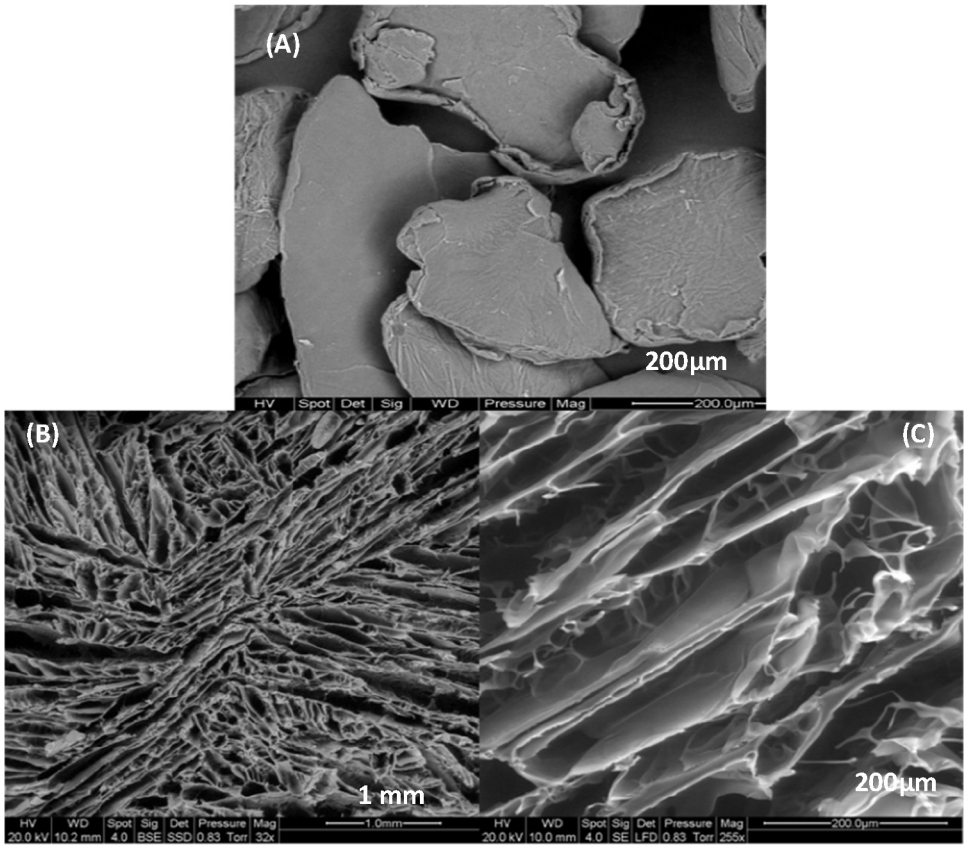

Fig. 3. SEM photographs of chitosan flakes (A) and foams (B) and (C) (scale bar: 200 μm (A), 1.0 mm (B), 200 μm (C)).

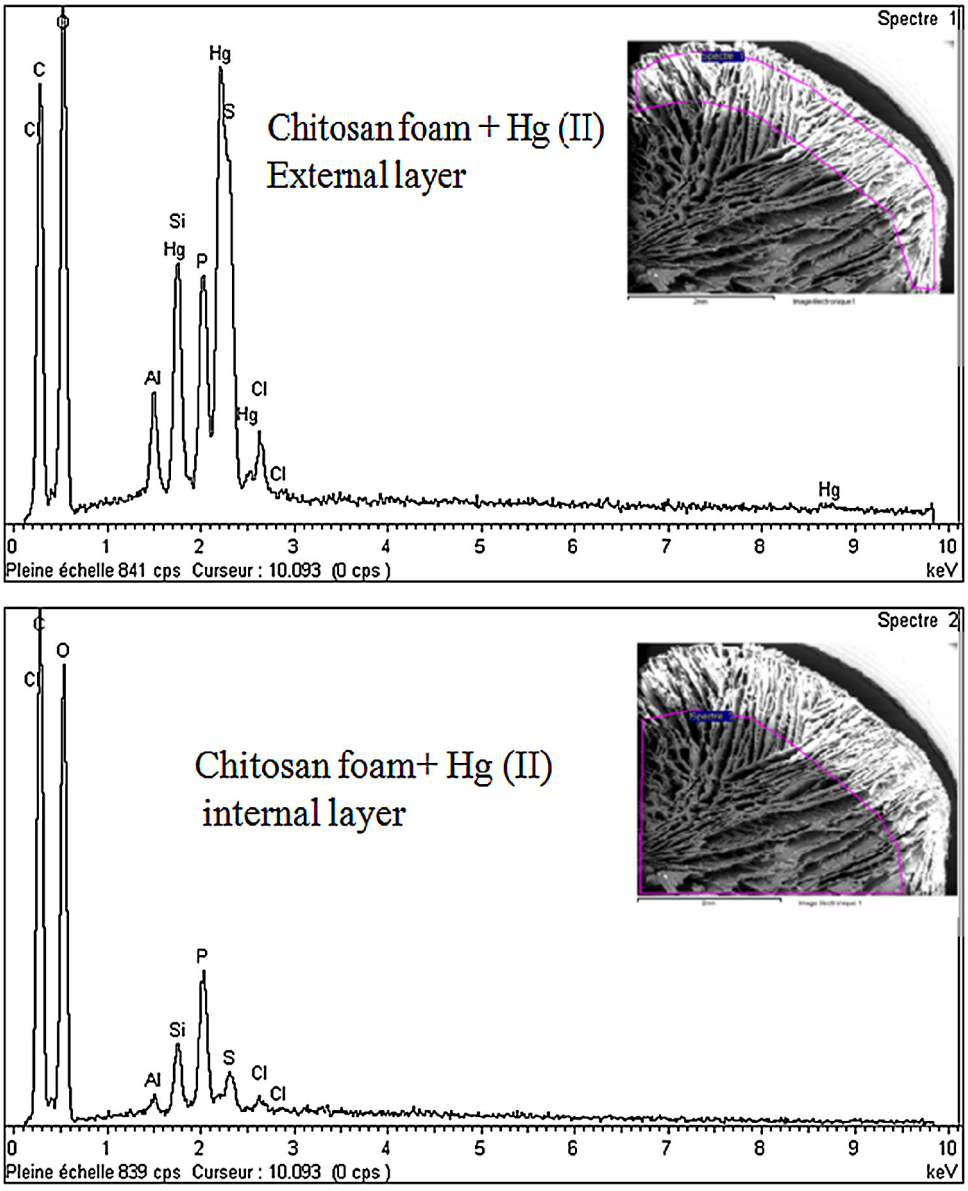

Fig. 4. SEM-EDAX analysis of chitosan foam after Hg(II) sorption—metal localization (framed zone corresponds to the surface area analyzed by EDAX).

Quanta FEG 200 equipped with an OXFORD Inca 350 mark Energy Dispersive X-ray microanalysis (EDX) system. The morphology, porosity, particle size and surface roughness of the chitosan were analyzed.

3. Results and discussion

3.1. Characterization of chitosan-based material

3.1.1. Photography observation

To improve the porosity of the chitosan and in order to achieve efficient sorption for mercury removal, chitosan under the form of cylindrical foams were prepared. The photography of chitosan foam provided in Fig. 1. shows a cylindrical shape (cylinder: 10 mm height and 10 mm diameter). It can be seen clearly that chitosan foam is well shaped as sponge-like and has smooth surfaces with many pores just visible to the naked eye.

3.1.2. SEM and SEM-EDX analyses

The Fig. 3(A) and (B) shows the observation by a scanning electron microscope of the chitosan G2 and chitosan foam, respectively. The micrograph of chitosan G2 shows an irregular flakes morphology while chitosan foams showed a uniform morphology and porous structure on the external layers at the micrometer scale (Fig. 3(B) and (C)). On the other hand, the free volume of cylindrical foams were determined preliminary using a pycnometer and the results were found not conclusive. The surface morphology of the cylindrical foam was examined and described an internal organization sponge-like structure with the presence of numerous cells and different pore size. In the current case, the average network openings seems to be between 1.0 mm and 200 μm at a higher magnitude (Fig. 3(B) and (C)).

The distribution of the pore volume on the chitosan foam is even more interesting, it allows us to understand the metal binding mechanisms and to determine the factors that control the uptake kinetics. After metal sorption, the distribution of mercury in the

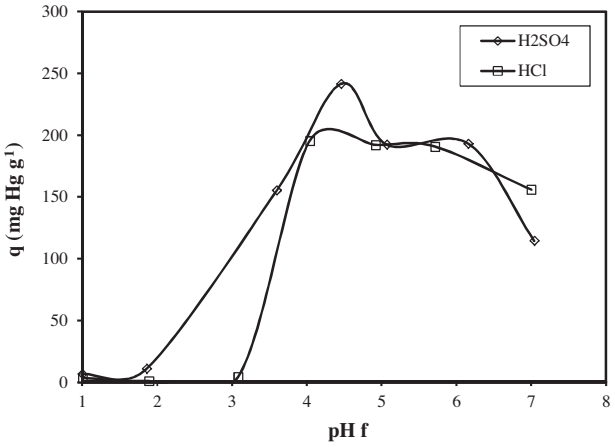

Fig. 5. Influence of pH on Hg(II) sorption using chitosan flakes (V: 100 mL; C_0: 50 mg Hg L^{-1}; Sorbent dosage: 0.20 g L^{-1}, PS:G2).

external surface and the central part of the chitosan-based material was performed using SEM-EDAX analysis (Fig. 4). The observation of the cylindrical section shows quite considerable variation of mercury concentration in the external and the central part of the material. The amount of Hg(II) is higher in the external layers than in the central part of the biopolymer materials. This implies that the metal solution–diffusion based material can be explained by: the diffusion limitation and incomplete saturation of the material. These results may indicate that chitosan flakes present higher capacity than foams, suggesting that the decrease is due to limitation of the metal ions accessibility on the internal functional groups. On the other hand, the results indicate that mercury sorption performance may depend on the ionic interactions and complex formation between metal cations and ligands present at the surface structure of the biomaterial. In the same manner that chitosan foams were prepared, Jouannin et al. [30] have obtained recently a comparable shape from alginate and tested as a catalyst support.

3.2. Effect of pH

The pH solution has an important effect on the sorption of mercury onto chitosan. Hence, the pH strongly control sorption performance (sorption isotherm) and the uptake mechanism (speciation of the metal, chelation and electrostatic attraction mechanism). Thus, chitosan is considered as a weak base, insoluble in water and characterized by its easy dissolution in many dilute mineral acids, with the remarkable exception of sulfuric acid solutions [31,32]. The results found in the literature concluded that chitosan becomes fully soluble below ~pH 5 or 6 in dilute aqueous acids [32,33]. Therefore, this factor must be considered carefully during the adsorption optimization process. In the present study, to prevent the chitosan dissolution, the effect of pH was carried as a function of metal sorption at different initial pHs range of 2–7, using hydrochloric and sulfuric acid (HCl, H_2SO_4). The adsorption behavior of Hg(II) on chitosan as a function of acidic solution is shown in Fig. 5. As mentioned from Fig. 5., chitosan is relatively stable in sulfuric acid solutions and mercury was present in the solution under the cationic form (Hg^{2+}). While with a presence of chloride acid, the sorption capacity decreased due to the ionization of $HgCl_2$ to form $HgCl_4^{2-}$. The sorption of mercury on chitosan was strongly affected by the pH of solution and was generally significantly decreased by increasing the pH, the highest uptake value achieved at pH 4.5. At pH 3 (and below), chitosan lost most of its sorption efficiency. When the pH >4.5, the metal ion seems to get out of the solution due to formation of colloidal precipitate of $Hg(OH)_2$ but not due to the adsorption of free Hg(II) ions. In general the uptake of Hg(II) at pH >6 is attributed to the formation of metal hydroxide species such as soluble $Hg(OH)^+$ and/or insoluble precipitate of $Hg(OH)_2$. Similarly, Xiong et al. [34], noted that the optimal sorption for mercury on cross-linked chitosan microspheres was obtained at pH 4.5. Otherwise, the protonation of amine groups is also responsible for chitosan dissolving in dilute acidic solutions (with the exception of sulfuric acid) [35]. However, the protonation of amine groups induced an electrostatic repulsion of metal cations and reduced the number of binding sites available for mercury sorption [35–37]. Consequently, the protonation causes the chitosan to dissolve, making it unsuitable for reuse. Moreover, in most cases, the metal cations can be adsorbed by chelation on amine groups of chitosan in near neutral solutions. According to our experiment, these results suggest that metal precipitation of mercury did not occur in all pH ranges as shown in Fig. 5. This result is in agreement with the data reported in previous studies [34,38,39]. The optimum pH of Hg(II) sorption is frequently reported in the literature to be around pH 4–6 (Table 2). In this study, taking into account the present results it appears that the optimum adsorption being closed at pH 4. All subsequent experiments were conducted at this pH value.

3.3. Adsorption equilibriums

The two most commonly familiar Langmuir and Freundlich models are used to describe the equilibrium isotherms for both chitosan G2 and cylindrical foams.

3.3.1. Langmuir isotherm

The Langmuir [40] isotherm based on mechanistic hypotheses can be written as:

$$q_e = \frac{q_m b C_e}{1 + bC_e} \tag{2}$$

In Eq. (1), q_e and q_m are the sorption capacity (mg g^{-1}) in equilibrium with concentration C_e (mg L^{-1}) and at saturation of the monolayer, respectively; b (L mg^{-1}) is the affinity coefficient of the sorbent. Its linear form can be expressed as: (Eq. (3))

$$\frac{1}{q_e} = \frac{1}{q_m} + \frac{1}{q_m b C_e} \tag{3}$$

3.3.2. Freundlich isotherm

Freundlich [41] isotherm was represented by the following Eq. (4):

$$q_e = k_F C_e^{1/n} \tag{4}$$

where K_F is the adsorption capacity parameter ($mg^{1-1/n}\,L^{1/n}\,g^{-1}$) and $1/n$ adsorption energy distribution parameter (unit less).

The linear form of Freundlich isotherm is given by the equation:

$$\ln q_e = \ln K_F + \left(\frac{1}{n}\right) \ln C_e \tag{5}$$

According to the adsorption equation, constant K_F indicates the chitosan sorption capacity when the concentration of adsorbate in the solution is equal to 1 mol L^{-1}. The coefficient $1/n$ represents the sorption intensity and adsorbent heterogeneity.

The fitting parameters of the two models are listed in Table 1, The high values of regression coefficients (R^2) confirm that the Langmuir model will better fit the experimental data than the Freundlich model. From the best correlation obtained by using Langmuir model, it can be concluded that the monolayer adsorption is more appropriate to explain the adsorption of Hg(II) and indicates at the same time that chemisorption might also be involved in the sorption process. From the Fig. 6, the adsorption isotherms were observed for both chitosan flakes and foam. Data showed a decrease in the amount of mercury capacity on chitosan

Table 1
Equilibrium constants for the adsorption of mercury onto chitosan fitted to the L–F isotherm model.

	Langmuir isotherm constants for adsorption of mercury onto chitosan		
	q_{mod} (mg g^{-1})	b (L mg^{-1})	R^2
Chitosan	850	0.034	0.995
Chitosan foam	350	0.062	0.970
	Freundlich isotherm constants for adsorption of mercury onto chitosan		
	n_f	K_F (mg g^{-1})	R^2
Chitosan	1.3	34.4	0.989
Chitosan foam	2.34	47.1	0.928

(Chitosan PS:G2).

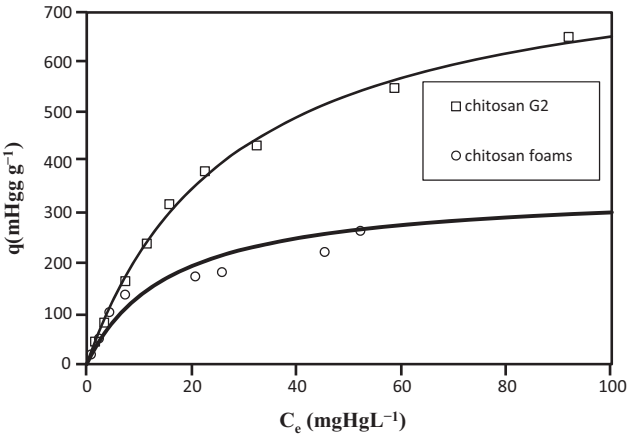

Fig. 6. Hg(II) sorption isotherms using chitosan G2 and foam—(solid line represents the modeling of experimental data with the Langmuir equation and the parameters reported in Table 1).

foam. Results obtained in (Fig. 6) indicate that the mercury sorption capacity on chitosan foam reached 350 mg Hg g^{-1}, while the sorption on chitosan G2 increased up to 850 mg Hg g^{-1}. Comparative and competitive biosorbents for mercury Hg(II) sorption are reported in Table 2. It can be seen that the qm value varies significantly for different biosorbents and that by comparison, the chitosan foam indicates a good capacity to adsorb Hg(II) ions from aqueous solutions. Generally, the maximum adsorption capacity depends on experimental conditions such as temperatures, adsorbent dose, pH,... etc. According to the published works [16,17,42], the sorption capacity of chitosan at raw form was higher than that of other form but despite that, several methods have been used to modify natural chitosan either physically or chemically in order to improve the sorption capacity especially in acidic condition. A useful comparison between results was reported in Table 3. It can be seen from Table 3, that the natural chitosan material used in this study, showed a good sorption affinity on Hg(II) without any modification or by grafting with new functional groups on the raw material. Zhou et al. [43,44] have shown that sorption capacity of mercury on natural chitosan at raw form is sometimes 3 to 4 times higher than the modified form of chitosan as beads, membranes or microspheres. . .etc. Similar observations were found for removal of Hg(II) on cross-linked magnetic chitosan-phenylthiourea resin [45] and on composite carbon nanotubes beads [46]. The behavioral differences for Hg(II) sorption on chitosan derivatives may be influenced by some key parameters such as the porosity and the specific surface area/mass ratio [47]. Also Kurita et al. and Vieira et al. [48,49] cites that crystallinity of chitosan can be considered as a one key parameter in the accessibility of internal sites for metallic ions and can improve adsorptive characteristics. It is important to note, that the cylindrical chitosan foams presented in this paper remains among the best biosorbent reported in the literature for

Table 2
Comparison of Hg(II) sorption onto different biosorbents.

Biosorbent	pH	Specific experimental conditions	q_m or q_{max} (mg Hg g^{-1})	Isotherm	Reference
Activated C from waste	–	30 °C	25.88	L	[12]
Marin macroalga	4.5	–	178	L	[6]
Cystoseira baccata	6		329		
Ulva lactuca	5.5	25 °C	84.7	L–F	[8]
Lessonia nigrescens	5	20 °C	157.3	L	[9]
	6		238.5		
	7		321.2		
Lessonia trabeculata	5	20 °C	170.7	L	[9]
	6		266.8		
	7		349.2		
Chlamydomonas reinhardtii	6	25 °C	72.2	L	[7]
Bacillus sp.	6	25 °C	7.9	L	[5]
Crab carapace	3	22 °C	13	–	[13]
Chitin	–	–	100	–	[21]
Chitosan	–	–	815	–	
Chitosan	4.5	25 °C	750	L	[22]
	6		1127		
Chitosan (PS:G2)	4	20 °C	850	L	Present study
Chitosan foams	4	20 °C	350	L	Present study

Table 3
Comparison of Hg(II) sorption on different synthesized chitosan materials.

Biosorbent	pH	Specific experimental conditions	q_m or q_{max} (mg Hg g^{-1})	Isotherm	Reference
Aminated chitosan beads	4	–	89	L	[39]
	7	–	496	L	
Cross-linked magnetic chitosan-phenylthiourea resin	5	30 °C	135	L	[45]
Composite carbon nanotubes beads	4	70 °C	172.7	L	[46]
Natural chitosan membrane	6	–	25.3	L	[47]
Glutaraldehyde-crosslinked chitosan	6	25 °C	75.5	L	
Natural chitosan spheres	6	–	13.5	L	
Glutaraldehyde-crosslinked chitosan spheres	6	–	31.1	L	
CG–MCS nano-absorbent	5–7	30 °C	285.71	L	[52]

their selectivity toward Hg(II). On the other hand, for the technical and economical approach the chitosan foams have an easy exploitation in continuous reactor, which makes it interesting for industrial applications, the choice is mainly related to the simplicity of the process design.

3.4. Sorption kinetics

Schematically, several diffusion mechanisms: (a) bulk diffusion, (b) film diffusion, and (c) intraparticle diffusion may control the kinetic sorption. In order to determine the best kinetic model which fits the experimental data sorption, two kinetic models were tested, including the pseudo-second-order [50] and Fick's diffusion kinetic models. It is generally accepted that pseudo-second-order model based on the sorption capacity of solid phase is the best data fits for describing the mechanism of mercury sorption on chitosan. Kinetics profiles were compared with theoretical curves based on solutions of Fick's diffusion equation and its simplified form.

3.4.1. Pseudo second order model

The pseudo-second order equation is based on the sorption capacity of the solid phase [50]. The pseudo-second order rate constant can be calculated from the following equation:

$$q_t = \frac{q_e^2 kt}{1 + q_e kt} \tag{6}$$

where K_2 is the pseudo second order rate constant ($g\,mg^{-1}\,min^{-1}$). After linearization:

$$\frac{t}{q_t} = \frac{1}{h} + \frac{1}{q_e} t \tag{7}$$

were q_t is the amount of Hg(II) adsorbed at time t $mg\,g^{-1}$ and q_e is experimental amount of metal adsorbed at equilibrium ($mg\,g^{-1}$); the k_2 and h can be determined from the slope and the intercept of the plot.

3.4.2. Fick's Second law of diffusion model

Equations based on Fick's law have been commonly used to model diffusion processes in biopolymers, pharmaceuticals, food science, nuclear materials. . .etc. In theory, Fick's second law predicts how diffusion causes the concentration to change with time, this equation is required to describe transport of components in materials when the endogenous sites are less accessible. Generally, the Fick's second law equations are used when the film diffusion or particle diffusion equations are less appropriate to fit the kinetic adsorption curves. For simple geometrical cases such as cylinder or sphere, the equation can be defined as follows:

$$\frac{q_t}{q_e} = 1 - b\exp(-kt) \tag{8}$$

where k, is the mass transfer coefficient (ms^{-1}), and b is the coefficient depending on experimental conditions. Whit a linear form of:

$$q_t = q_e(1 - b\exp(-kt)) \tag{9}$$

3.4.3. Effect of initial metal concentration (C_0)

The results for Hg(II) sorption on chitosan flakes (PS:G2 chitosan and 20 °C) are plotted in Fig. 7. Data shows an increase in sorption of Hg(II) with an increase in the initial metal concentration (C_0) from 25 to 100 mg Hg L^{-1}. Three distinct regions can be distinguished by observation of the curve: (1) sorption increases rapidly at the beginning which indicates the instantaneous sorption suggesting rapid external diffusion and surface adsorption; (2) sorption increases gradually with time resulting from chemical reactions (3) the equilibrium state indicates that the sorbent reached saturation. Therefore, the highest sorption capacity at concentration of

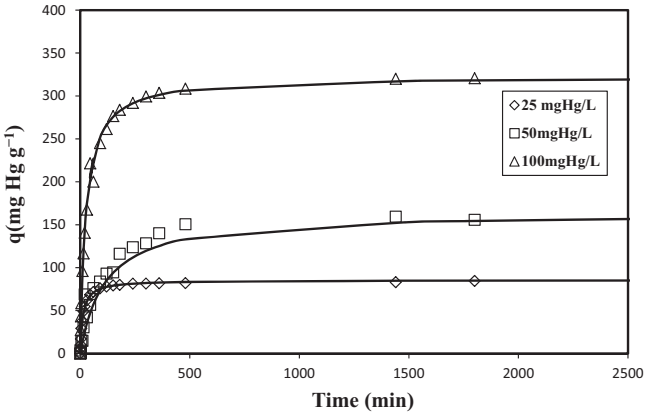

Fig. 7. Influence of initial metal concentration (C_0, mg Hg L^{-1}) on Hg(II) uptake kinetics (pH 4; SD: 0.625 g L^{-1}; C_0: mg Hg L^{-1}; PS:G2; curves represent the modeling of uptake kinetics with the PSORE).

100 mg L^{-1} of Hg(II) is probably due to the quasi-saturation of the sorbent. The sorption equilibrium was reached after 3 h, depending on the initial metal ion concentration. It was also suggested that the binding affinity of metal within the pores of chitosan material as result of an increasing of the time of the sorption process. The pseudo-second order model has been successfully used to fit the kinetic data, suggesting chemical adsorption as the rate-limiting step of the adsorption mechanism involving chemisorption, where metal removal from solution is due to purely physicochemical interactions between sorbent and sorbate. The sorption of Hg(II) using chitosan G2 was significantly faster in batch reactor stirrer. Table 4, presents the kinetic parameters for adsorption of Hg(II) on chitosan G2 resulted by fitting the pseudo-second order equation to the experimental data. Note that, the rate constant, k_2, was found to increase at low concentration of Hg(II).

Much of the published studies have demonstrated that the pseudo-second order model has been successfully used to fit the kinetic data of Hg(II) on chitosan-coated cotton fibers [51], Hg(II) ions by thiourea-modified magnetic chitosan microspheres [44] Hg(II) on multi-cyanoguanidine modified magnetic chitosan [52] and Hg(II) on chitosan cross-linked with a barbital derivative [53].

3.4.4. Column sorption

Until now, to overcome the reduction in friction loss and column clogging caused by using chitosan flakes or powder, several research works propose to prepare chitosan in a useful form to improve design of biosorption system [31,47]. The results of cylindrical chitosan foams placed in a column at three initial concentration of metal, and by varying bed depth and flow rate (results not shown) as a function of time are shown in Figs. 8 and 9, respectively. The results of uptake kinetic experiments show as the bed depth increase, the residence time of the fluid inside the column increases. It is apparent from Fig. 8(a)–(c) that all the curves present a similar shape, the plots could be split in two distinct steps: In the first step, the sorption process is relatively faster and corresponds to the pseudo-plateau, which is attributed to the sorption of metal

Table 4
Parameters of the pseudo-second order rate equation for adsorption of Hg(II) on chitosan G2 with different initial concentration.

	Pseudo-second order model			
C_0 (mg L^{-1})	q_{exp}	q_{mod}	K_2	R^2
25	85.4	83.7	9.5×10^{-4}	0.999
50	163.93	157.8	5.46×10^{-4}	0.964
100	322.5	319.7	1.2×10^{-4}	0.999

Chitosan (PS:G2), q: mg Hg g^{-1}; k_2: g mg^{-1} min^{-1}.

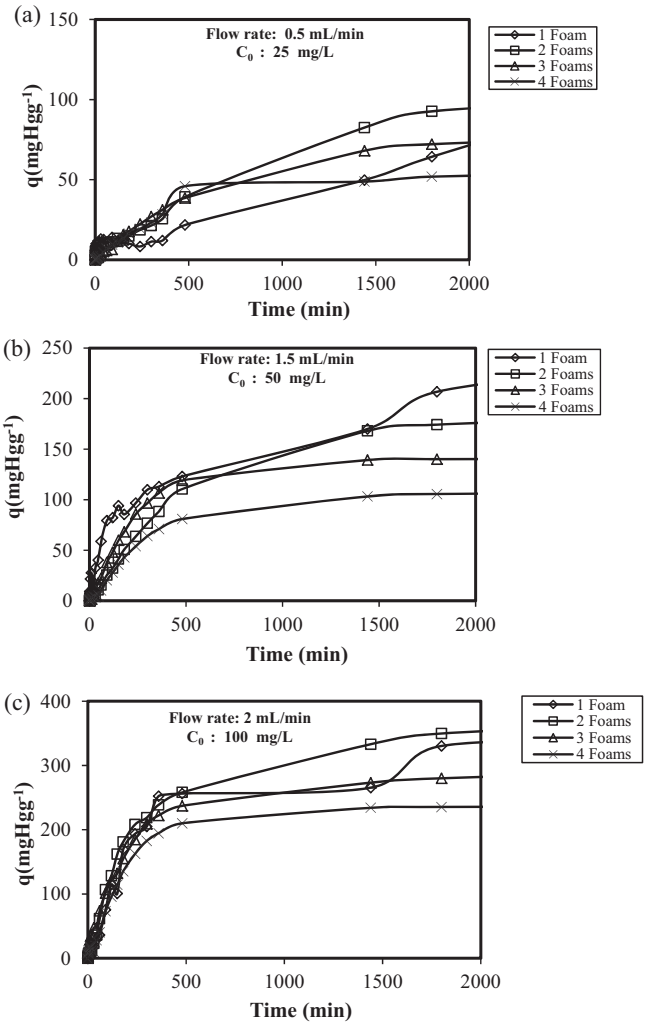

Fig. 8. Influence of flow rate and initial metal concentration (C_0, mg Hg L^{-1}) on Hg(II) uptake kinetics chitosan foams ((a) 25 mg L^{-1}; (b) 50 mg L^{-1};(c) 100 mg L^{-1}).

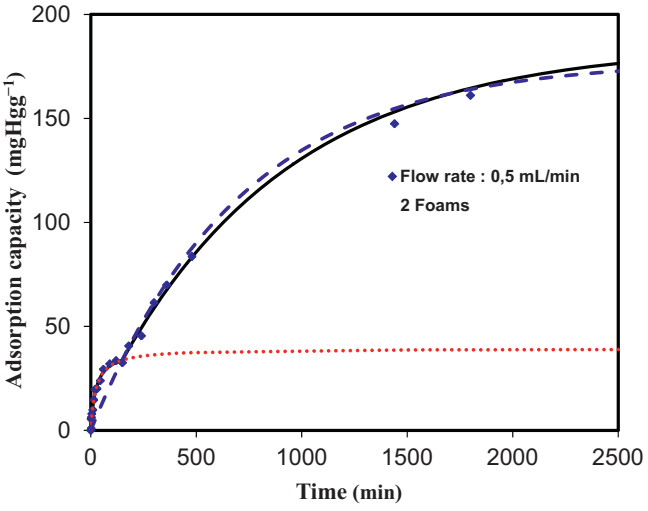

Fig. 9. Influence of flow rate on the sorption capacity of chitosan foam (pH 4; C_0:50 mg L^{-1}; T: 20 °C; flow rate: 0.5 mL min^{-1}; curves represent the modeling of uptake kinetics: on the first panel red line shows the modeling of curve with the model PSORE and the blue solid line shows the modeling of curve with the cylindrical mass transfer model.

Table 5
Parameters of kinetics model for adsorption of Hg(II) on chitosan foam with different initial concentration.

Pseudo-second order model				
Flow rate	C_0 (mg L^{-1})	q_{exp}	K_2	R^2
0.5	25	35	3.08×10^{-4}	0.399
0.5	50	39.3	1.05×10^{-3}	0.977
0.5	100	160	2.22×10^{-5}	0.887
		Fick's second law		
0.5	25	111	8.92×10^{-4}	0.975
0.5	50	178	1.41×10^{-3}	0.976
0.5	100	185	1.83×10^{-3}	0.982

q: mg Hg g^{-1}; k_2: gmg^{-1} min^{-1}; k (m/s).

ions on the most active binding sites of the biopolymer, followed by a saturation plateau. This corresponds to the second slow step which is probably controlled by diffusion and involves the binding of metal on the lower energy sites and increases the accessibility to internal site of the cylindrical foams. It also appears from Fig. 8, that the flow rate had a limited impact on kinetic sorption. This phenomenon was observed at all low concentration and low flow rate and concealed relatively at higher flow rate or higher concentration, because in both cases the amount of metal upon surface contact of the solid phase increases and the first step is considered almost instantaneous. It is noteworthy that the amount of metal retained in this first step may not exceed 10% of the total amount of metal (Fig. 9).

However, taking into account the sorbent geometry, a cylindrical diffusion model was used to simulate uptake curve. This model was evaluated with regard to its ability to describe slow uptake. From the kinetic profile, two regions seem to be observed before and after the pseudo-plateau: (i) For the first region a pseudo-second order model has been applied successfully to metal sorption and also allowed fast sorption kinetics, (ii) On the second region, the cylindrical mass transfer model based on diffusion will be applied to fit experimental data and hence the mass transfer represent the rate-limiting step (Fig. 9). In other words, this second slow step seems to be related to the binding of the metallic ions or diffusion within the pores of foams and the interaction of metal with the available sorption sites on the inside of the foam. Based on the results of kinetic, good fits between predicted curves and experimental values were found with both model in the present study. The kinetic parameters of Hg(II) biosorption onto chitosan foam are reported in Table 5. Accordingly as shown in Tables 4 and 5, the pseudo-second-order rate constant (k_2) of chitosan G2 was higher than the coefficient obtained with chitosan foam. The diffusion coefficient was more significantly changed by an increase in the initial concentration of Hg(II). In general, the differences were not as marked as they were with some chitosan derivatives [52–55].

4. Conclusions

In the present study a natural chitosan sponge-like material has been prepared and characterized. SEM images revealed a regular morphology and porous structure. Obviously, further work with the use of BET-surface analysis during sorption would be very useful in order to better define the porous structure of this material. In this first attempt, to improve the Hg(II) sorption efficiency on our materials, we have studied the sorption capacity of Hg(II) in a column on recirculation-flow operation: The mercury sorption capacity on the cylindrical foam reached 350 mg Hg g^{-1}, while for chitosan (G2) increased up to 850 mg Hg g^{-1} at batch system. The sorption data follows Langmuir model and the monolayer adsorption was dominated. Kinetic data was successfully fitted to pseudo-second order model for short sorption time. This phenomenon indicates that chemical adsorption was the rate-control step, while the cylindrical diffusion model was able to predict the end of the

sorption. The combination of these two models is usually helpful for predicting the whole set of data at equilibrium. Finally, column results, indicate that the chitosan conditioned under the form of cylindrical foam is considered as an encouraging material from laboratory tests to industrial application compared to other biosorbent reported in the literature for their selectivity toward Hg(II).

Acknowledgments

This research was financially supported by Grant PNE (Programme National Exceptionnel, Ministère de l'Enseignement Supérieur et de la Recherche Scientifique—Algérie). The authors acknowledge the personal J.-M. Taulemesse (from Centre des Matériaux de Grande Diffusion, Ecole des Mines d'Alès) for SEM/SEM-EDAX. Sincere thanks go to Pr E- Benyoussef (from Ecole Nationale Polytechnique—Alger).

References

[1] World Health Organization (W.H.O), Mercury in drinking-water. Guidelines for drinking-water quality Recommendations, 1, second ed., World Health Organization (W.H.O), Geneva, 1993, ISBN 92 4 154460.
[2] F-N. Allouche, N. Mameri, E. Guibal, Pb(II) biosorption on *Posidonia oceanica* biomass, Chem. Eng. J. 168 (2011) 1174–1184.
[3] E. Guibal, K.C. Gavilan, P. Bunio, T. Vincent, A. Trochimczuk, I.L101 Cyphos, (Tetradecyl (Trihexyl) Phosphonium Chloride) immobilized in biopolymer capsules for Hg(II) recovery from HCl solutions, Sep. Sci. Technol. 43 (2007) 2406–2433.
[4] A. Kapoor, T. Viraraghavan, Fungal biosorption—an alternative treatment option for heavy metal bearing wastewaters: a review, Bioresour. Technol. 53 (1995) 195–206.
[5] K. Kapoor, Y-S. Yun, Bacterial biosorbents and biosorption, Biotechnol. Adv. 26 (2008) 266–291.
[6] C. Green-Ruiz, Mercury(II) removal from aqueous solutions by nonviable *Bacillus* sp. from a tropical estuary, Bioresour. Technol. 97 (2006) 1907–1911.
[7] R. Herrero, P. Lodeiro, C. Rey-Castro, T. Vilarino, M. Sastre, de Vicente, Removal of inorganic mercury from aqueous solutions by biomass of the marine macroalga *Cystoseirabaccata*, Water Res. 39 (2005) 3199–3210.
[8] İ. Tüzün, G. Bayramoğlu, E. Yalçin, G. Başarana, G. Çelik, M.Y. Arıca, Equilibrium and kinetic studies on biosorption of Hg(II), Cd(II) and Pb(II) ions onto microalgae *Chlamydomonasreinhardtii*, J. Environ. Manage. 77 (2005) 85–92.
[9] Y. Zeroual, A. Moutaouakkil, F.Z. Dzairi, M. Talbi, P.U. Chung, K. Lee, Biosorption of mercury from aqueous solution by *Ulvalactuca* biomass, Bioresour. Technol. 90 (2003) 349–351.
[10] M. Reategui, H. Maldonado, M. Ly, E. Guibal, Mercury(II) Biosorption Using *Lessonia* sp. Kelp, Appl. Biochem. Biotechnol. 162 (2010) 805–822.
[11] E. Romera, F. Gonzalez, A. Ballester, M.L. Blăzquez, J.A. Muñoz, Comparative study of biosorption of heavy metals using different types of algae, Bioresour. Technol. 98 (2007) 3344–3353.
[12] L. Carro, J.L. Barriada, R. Herrero, M.E. Sastre de Vicente, Adsorptive behaviour of mercury on algal biomass: competition with divalent cations and organic compounds, J. Hazard. Mater. 192 (2011) 284–291.
[13] M.M. Rao, D.H.K. Kumar Reddy, P. Venkateswarlu, K. Seshaiah, Removal of mercury from aqueous solutions using activated carbon prepared from agricultural by-product/waste, J. Environ. Manage. 90 (2009) 634–643.
[14] I.B. Rae, S.W. Gibb, S. Lu, Biosorption of Hg from aqueous solutions by crab carapace, J. Hazard. Mater. 164 (2009) 1601–1604.
[15] A. Bhatnagar, M. Sillanpää, Utilization of agro-industrial and municipal waste materials as potential adsorbents for water treatment—a review, Chem. Eng. J. 157 (2010) 277–296.
[16] R. Bassi, S.-O. Prasher, B.-K. Simpson, Removal of selected metal ions from aqueous solutions using chitosan flakes, Sep. Sci. Technol. 35 (2000) 547–560.
[17] M.-S. Dzul Erosa, T.-I. Saucedo medina, R. Navarro Mendoza, M. Avila Rodriguez, E. Guibal, Cadmium sorption on chitosan sorbents: kinetic and equilibrium studies, Hydrometallurgy 61 (2001) 157–167.
[18] J.C.Y. Ng, W.H. Cheung, G. McKay, Equilibrium studies of the sorption of Cu(II) ions onto chitosan, J.Colloid Interface Sci. 255 (2002) 64–74.
[19] R-N. Shinde, A.K. Pandey, R. Acharya, R. Guin, S.K. Das, N.S. Rajurkar, P.K. Pujari, Chitosan-transition metal ions complexes for selective arsenic(V) preconcentration, Water Res. 47 (2013) 3497–3506.
[20] F. Condi de Godoi, E. Rodriguez-Castellon, E. Guibal, M.-M. Beppu, An XPS study of chromate and vanadate sorption mechanism by chitosan membrane containing copper nanoparticles, Chem. Eng. J. 234 (2013) 423–429.
[21] S.E. Bailey, T.J. Olin, R.M. Bricka, D. Adrian, A review of potentially low-cost sorbents for heavy metals, Water Res. 33 (1999) 2469–2479.
[22] A. Shafaei, F.Z. Ashtiani, T. Kaghazchi, Equilibrium studies of the sorption of Hg(II) ions onto chitosan, Chem. Eng. J. 133 (2007) 311–316.
[23] E. Guibal, C.A. Milot, O.B. Erradossi, C.C.A. Gauffier, Domard, study of molybdate ion sorption on chitosan gel beads by different spectrometric analyses, Inter, J. Biol. Macromol. 24 (1999) 49–59.
[24] C. Jeon, K-H. Park, Adsorption and desorption characteristics of mercury(II) ions using aminated chitosan bead, Water Res. 39 (2005) 3938–3944.
[25] I.S. Arvanitoyannis, A. Nakayama, S. Aiba, Chitosan and gelatin based edible films: state diagrams, mechanical and permeation properties, Carbohydr. Polym. 37 (1998) 371–382.
[26] R.S. Vieira, M.L.M. Oliveira, E. Guibal, E. Rodríguez-Castellón, M.M. Beppu, Copper, mercury and chromium adsorption on natural and crosslinked chitosan films: an XPS investigation of mechanism, Colloids Surf., A 374 (2011) 108–114.
[27] T. Vincent, E. Guibal, Chitosan-supported palladium catalyst. 5. Nitrophenol degradation using palladium supported on hollow chitosan fibers, Environ. Sci. Technol. 38 (2004) 4233–4240.
[28] C. Liu, R. Bai, Preparing highly porous chitosan/cellulose acetate blend hollow fibers as adsorptive membranes: effect of polymer concentrations and coagulant compositions, J. Membr. Sci. 279 (2006) 336–346.
[29] E. Guibal, C. Milot, J.M. Tobin, Metal-anion sorption by chitosan beads: equilibrium and kinetic studies, Ind. Eng. Chem. Res. 37 (1998) 1454–1463.
[30] C. Jouannin, I. Dez, A-C. Gaumont, J.M. Taulemesse, T. Vincent, E. Guibal, Palladium supported on alginate/ionic liquid highly porous monoliths: application to 4-nitroaniline hydrogenation, Appl. Catal., B 103 (2011) 444–452.
[31] E. Guibal, Interactions of metal ions with chitosan-based sorbents: a review, Sep. Purif. Technol. 38 (2004) 43–74.
[32] G. Crini, P-M. Badot, Application of chitosan, a natural aminopolysaccharide, for dye removal from aqueous solutions by adsorption processes using batch studies: a review of recent literature, Prog. Polym. Sci. 33 (2008) 399–447.
[33] C.K.S. Pillai, Willi Paul, P. Chandra, Sharma, Chitin and chitosan polymers: chemistry, solubility and fiber formation, Prog. Polym. Sci. 34 (2009) 641–678.
[34] C. Xiong, L. Pi, X.Chen L. Yang, C. Ma, X. Zheng, Adsorption behavior of Hg^{2+} in aqueous solutions on a novel chelating cross-linked chitosan microsphere, Carbohydr. Polym. 98 (2013) 1222–1228.
[35] G.A.F. Roberts, Chitin Chemistry, first ed., Macmillan, London, 1992.
[36] W.S. Wan Ngah, C.S. Endud, R. Mayanar, Removal of copper(II) ions from aqueous solution onto chitosan and cross-linked chitosan beads, React. Funct. Polym. 50 (2002) 181–190.
[37] C. Jeon, W.H. Höll, Chemical modification of chitosan and equilibrium study for mercury ion removal, Water Res. 37 (2003) 4770–4780.
[38] A-M. Donia, A-A. Atia, K-Z. Elwakeel, Selective separation of mercury(II) using magnetic chitosan resin modified with Schiff's base derived from thiourea and glutaraldehyde, J. Hazard. Mater. 151 (2008) 372–379.
[39] L. Wang, R. Xing, S. Liu, S. Cai, H. Yu, J. Feng, R. Li, P. Li, Synthesis and evaluation of a thiourea-modified chitosan derivative applied for adsorption of Hg(II) from synthetic wastewater, Int. J. Biol. Macromol. 46 (2010) 524–528.
[40] I. Langmuir, The constitution and fundamental properties of solids and liquids, J. Am. Chem. Soc. 38 (1916) 2221–2295.
[41] H.M.F. Freundlich, Over the adsorption in solution, Z. Phys. Chem. 57A (1906) 385–470.
[42] P. Miretzky, A.F. Cirelli, Hg(II) removal from water by chitosan and chitosan derivatives: a review, J. Hazard. Mater. 167 (2009) 10–23.
[43] L.M. Zhou, S.R. Liu, Q.W. Huang, Adsorption of mercury and uranyl onto poly(ethyleneimine) grafted chitosan microspheres, Mod. Chem. Ind. 27 (2007) 175–177.
[44] L. Zhou, Y.Z. Wang, Q.W. Liu Huang, Characteristics of equilibrium, kinetics studies for adsorption of Hg(II), Cu(II), and Ni(II) ions by thiourea-modified magnetic chitosan microspheres, J. Hazard. Mater. 161 (2009) 995–1002.
[45] M. Monier, D.-A. Abdel-Latif, Preparation of cross-linked magnetic chitosan-phenylthiourea resin for adsorption of Hg(II), Cd(II) and Zn(II) ions from aqueous solutions, J. Hazard. Mater. 209–210 (2012) 240–249.
[46] H-A. Shawky, A.M. El-Aassar, D.E. Abo-Zeid, Chitosan/carbon nanotube composite beads: preparation, characterization, and cost evaluation for mercury removal from wastewater of some industrial cities in Egypt, J. Appl. Polym. Sci. 125 (2012) 93–101.
[47] R.-S. Vieira, M.-M. Beppu, Dynamic and static adsorption and desorption of Hg(II) ions on chitosan membranes and spheres, Water Res. 40 (2006) 1726–1734.
[48] K. Kurita, T. Sannan, Y. Iwakura, Studies on Chitin. VI. Binding of metal cations, J. Appl. Polym Sci. 23 (1979) 511–515.
[49] R-S. Vieira, M-M. Beppu, Mercury ion recovery using natural and crosslinked chitosan membranes, Adsorption 11 (2005) 731–736.
[50] Y.S. Ho, G. MacKay, Pseudo-second order model for sorption processes, Process Biochem. 34 (1999) 451–465.
[51] R. Qu, C. Sun, F. Ma, Y. Zhang, C. Ji, Q. Xu, C. Wang, H. Chen, Removal and recovery of Hg(II) from aqueous solution using chitosan-coated cotton fibers, J. Hazard. Mater. 167 (2009) 717–727.
[52] Y. Wang, Y. Qi, Y. Li, J. Wu, X. Ma, C. Yu, L. Ji, Preparation and characterization of a novel nano-absorbent based on multi-cyanoguanidine modified magnetic chitosan and its highly effective recovery for Hg(II) in aqueous phase, J. Hazard. Mater. 260 (2013) 9–15.
[53] F. Ma, R. Qu, C. Sun, C. Wang, C. Ji, Y. Zhang, P. Yin, Adsorption behaviors of Hg(II) on chitosan functionalized by amino-terminated hyperbranched polyamidoamine, polymers, J. Hazard. Mater. 172 (2009) 792–801.
[54] S. Kushwaha, P-P. Sudhakar, Adsorption of mercury(II), methyl mercury(II) and phenyl mercury(II) on chitosan cross-linked with a barbital derivative, Carbohydr. Polym. 86 (2011) 1055–1062.
[55] J-D. Merrifield, W-G. Davids, J-D. Mac Rae, A. Amirbahman, Uptake of mercury by thiol-grafted chitosan gel beads, Water Res. 38 (2004) 3132–3138.